



# Dissipative and Autonomous Square-Wave Self-Oscillation of a Macroscopic Hybrid Self-Assembly under Continuous Light Irradiation

Tomonori Ikegami, Yoshiyuki Kageyama,\* Kazuma Obara, and Sadamu Takeda\*

**Abstract:** Building a bottom-up supramolecular system to perform continuously autonomous motions will pave the way for the next generation of biomimetic mechanical systems. In biological systems, hierarchical molecular synchronization underlies the generation of spatio-temporal patterns with dissipative structures. However, it remains difficult to build such self-organized working objects via artificial techniques. Herein, we show the first example of a square-wave limit-cycle self-oscillatory motion of a noncovalent assembly of oleic acid and an azobenzene derivative. The assembly steadily flips under continuous blue-light irradiation. Mechanical self-oscillation is established by successively alternating photoisomerization processes and multi-stable phase transitions. These results offer a fundamental strategy for creating a supramolecular motor that works progressively under the operation of molecule-based machines.

There is considerable interest in macroscopically active materials and molecular robots generated by the incorporation of functional molecules.<sup>[1–6]</sup> A key milestone in the mimicry of biological processes is the development of dissipative dynamics<sup>[7]</sup> that show continuous and macroscopically patterned motions with dissipation of supplied energy via self-organization, but without the motion being trapped in a potential minimum.<sup>[1]</sup> A typical phenomenon is self-oscillation, in which spatio-temporally patterned dynamics under the steady, but far-from-equilibrium, condition are generated by cooperative interactions within the system.<sup>[1,8]</sup> To date, oscillatory working polymer gels have been realized by using the Belousov-Zhabotinsky reaction.<sup>[9,10]</sup> We aim to develop autonomous, artificial, and supramolecular motions in an open system mimicking stimulus-responsive biological systems. For this reason, we prefer to construct the dissipative

motions of macroscopic supermolecules triggered by small functional molecules, or so-called molecular machines.<sup>[1,2]</sup>

Herein, we show the first example of a macroscopic square-wave, self-oscillatory motion of a noncovalent assembly of oleic acid and an azobenzene derivative. The assembly flips repeatedly in an autonomous manner under continuous blue-light irradiation, as shown in Figure 1 and Movies S1–S3 in the Supporting Information (SI). Mechanical self-oscillation is established by successively alternating photoisomerization processes and multi-stable phase transitions.

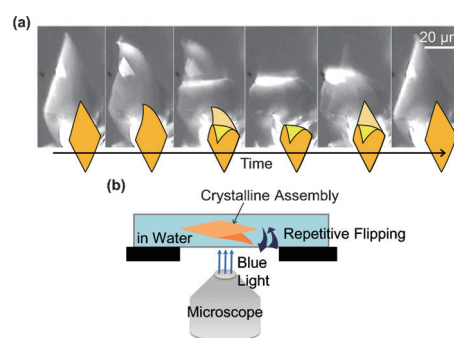


**Figure 1.** a) Sequential micrographs (40× objective lens, scale bar is 20 μm) of one cycle of self-oscillation observed under 435-nm light, taken from Movie S1, and their schematic illustrations. b) Schematic illustration showing setup for the observation of blue-light-induced self-oscillation.

Azobenzenes have frequently been employed in the creation of photomechanically working objects<sup>[3–5,11]</sup> and patterned dynamics.<sup>[12,13]</sup> Azobenzene is isomerized from the *trans* to *cis* form by ultraviolet (UV) irradiation. Reverse isomerization is achieved through a thermal process or blue-light irradiation. This photoisomerization alters the volume of azobenzene and the orientation of the transition dipole moment. Repeatable macroscopic dynamics of azobenzene-containing materials have been realized by altering the wavelength of applied light or by coupling photo and thermal processes.<sup>[3–5]</sup>

On the other hand, because blue light can induce *trans*-to-*cis* isomerization, repeated *trans*-to-*cis* and *cis*-to-*trans* photoisomerization events occur stochastically under blue-light irradiation. This property has been applied to create continuous working objects under photostationary-state (PSS) conditions. Credi and co-workers demonstrated the repetitive unidirectional transit of a macrocycle of azobenzene-pseudorotaxane in solution under the PSS condition, in the absence of macroscopically synchronized transient dynam-

[\*] Dr. Y. Kageyama, K. Obara, Prof. S. Takeda  
Department of Chemistry, Faculty of Science  
Hokkaido University  
Sapporo, 060-0810 (Japan)  
E-mail: y.kageyama@mail.sci.hokudai.ac.jp  
stakeda@sci.hokudai.ac.jp

Dr. Y. Kageyama  
JST PRESTO  
Kawaguchi, 332-0012 (Japan)  
T. Ikegami  
Graduate School of Chemical Sciences and Engineering, Hokkaido University  
Sapporo, 060-0810 (Japan)

Supporting information and the ORCID identification number(s) for the author(s) of this article can be found under <http://dx.doi.org/10.1002/anie.201600218>.

ics.<sup>[14]</sup> In contrast to an isotropic solution, repeated photoisomerization under polarized blue light results in a molecular ordering of azobenzene in condensed materials. Two-dimensional patterns have been formed on azobenzene-containing substrate surfaces<sup>[12]</sup> or amphiphilic azobenzene monolayer membranes.<sup>[13]</sup> Photo-driven oscillatory flipping of an azobenzene-polymer film could be produced by adjusting the direction of the incident polarized blue light, such that two sides of a film receive incident light alternatively owing to its flipping motion.<sup>[11]</sup> Herein, employing an entirely novel strategy, we achieved periodic flipping motions of azobenzene-containing noncovalent self-assemblies in aqueous dispersion in a dissipative and autonomous manner under continuous irradiation of nonpolarized blue light.

A mixed dispersion of an amphiphilic azobenzene (6-[4-(4-*n*-butylphenylazo)phenoxy]hexanoic acid, **1**) and sodium oleate (**2**) in a 4:6 molar ratio in phosphate-buffered solution

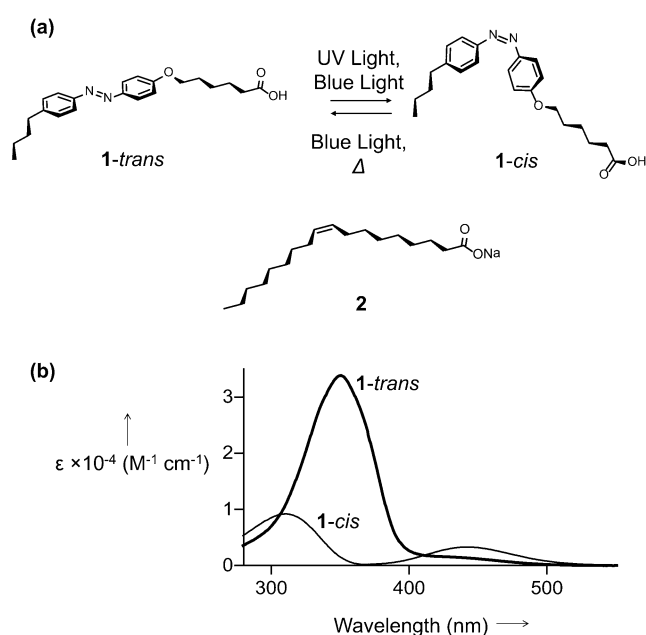


**Figure 2.** a) Schematic illustration of the molecular structures of **1** and **2**, and the photoisomerization reaction of **1**. b) UV/Vis absorption spectra of **1-trans** and **1-cis** in methanol. The absorption coefficient ( $\epsilon$ ) of **1-cis** was calculated from UV/Vis absorption spectra of a mixed solution of **1-trans** and **1-cis**, and from HPLC analysis of the mixed solution.

**Table 1:** Photochemical properties of **1** in methanolic solution.

Wavelength	$\epsilon_{\text{trans}} [\text{M}^{-1} \text{ cm}^{-1}]$	$\epsilon_{\text{cis}} [\text{M}^{-1} \text{ cm}^{-1}]^{[a]}$	<i>trans-cis</i> ratio in PSS <sup>[b]</sup>
435 nm	$1.44 \times 10^3$	$2.8 \times 10^3$	72:28
455 nm	$1.10 \times 10^3$	$2.7 \times 10^3$	76:24 <sup>[c]</sup>
470 nm	$0.75 \times 10^3$	$2.0 \times 10^3$	78:22

[a] Values calculated from UV/Vis absorption spectra of a mixed solution of **1-trans** and **1-cis**, and from HPLC analysis of the mixed solution.

[b] Values obtained from HPLC analysis of a 0.372 mM methanolic solution of **1** under PSS. Quantum yields of *trans*-to-*cis* and *cis*-to-*trans* at 435 nm were  $0.48 \pm 0.02$  and  $0.59 \pm 0.03$ , respectively, with the same values being obtained at 470 nm. Experimental details are described in the Supporting Information. [c] Using a handheld LED lamp as a light source, the ratio was 75:25, as shown in Figure 4d.

(pH 7.5, 75 mM) was refrigerated (4°C) for several days and allowed to form thin crystalline assemblies (Figure 2a). UV/Vis absorption spectra and photoisomerization properties of the *trans*- and *cis*-isomers of **1** in methanol are shown in Figure 2b and Table 1. An in situ small-angle X-ray diffraction (SAXRD) experiment indicated that the *d*-spacing of the assemblies in the aqueous dispersion was 4.6 nm ( $q = 1.37 \text{ nm}^{-1}$ ; Figure 3a).<sup>[15]</sup> Based on data from high-perfor-

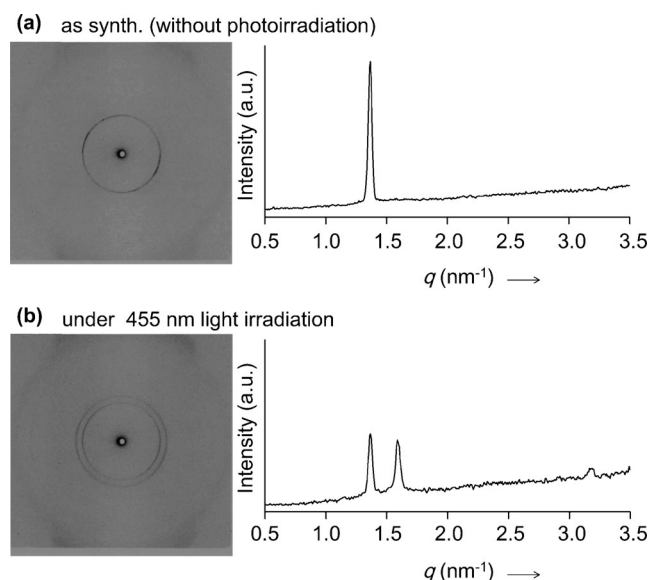


**Figure 3.** In situ SAXRD fringe images and profiles of assemblies measured a) in the dark, and b) under continuous 455-nm light irradiation.

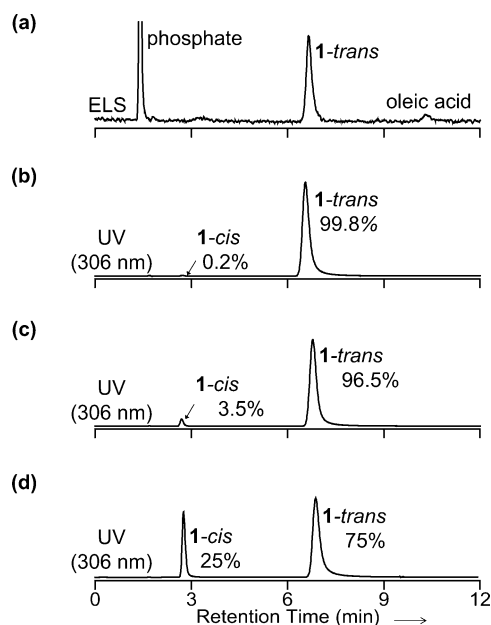


**Figure 4.** HPLC analyses. Chromatographs of assemblies as synthesized in the dark, recorded using the a) ELS detector and b) UV detector (monitored at 306 nm, an isosbestic point of **1-trans** and **1-cis**). c) Chromatograph of assemblies after 455-nm light irradiation. d) Chromatograph of a methanolic solution of **1** after 455-nm light irradiation.

mance liquid chromatography (HPLC) analysis with UV/Vis and evaporative light scattering (ELS) detectors (Figure 4a), we determined that the assembly is in a 6:4 molar ratio of **1** to **2**. The *d*-spacing value and composition ratio remained constant when the preparation was made with a 2:8 or 1:9 molar ratio mixture of **1** and **2**, indicating that the assembly was stoichiometrically uniform.<sup>[16]</sup> Fourier transform infrared (FTIR) microspectrometry yielded a strong peak at  $1706\text{ cm}^{-1}$ , which we assigned to the stretching mode of the hydrogen-bonded carboxyl groups (Figure S1 in SI). These results suggest that this crystalline assembly has a lamellar structure, in sharp contrast to our previously obtained photo-driven soft liquid crystals composed of **1** and **2**.<sup>[5,17]</sup> Using a differential interference contrast (DIC) microscope equipped with a high-pressure mercury lamp in its fluorescent unit, we found an oscillatory bending-unbending motion of the crystalline assembly of around  $1\text{ }\mu\text{m}$  in thickness under nonpolarized 435-nm light irradiation (Figure 1, and Movie S1 in SI). The frequency of the motion increased with increasing light intensity. A similar oscillation was observed under 470-nm light irradiation, but the assembly collapsed under 365-nm light irradiation.<sup>[18]</sup>

Figure 5a shows the time profile of oscillation for our plate-like crystalline assembly captured by a high-speed camera (1000 fps) under 435-nm light irradiation (Movie S2). The oscillation cycle consisted of four steps: sluggish bending of the flat assembly (S1), rapid morphological change of the assembly to a bent form (S2), sluggish unbending of the assembly (S3), and rapid return to the original morphology (S4). The time span of each step  $S_n$  is presented in the form  $\tau_n$ . The displacement magnitude for each step remained constant with changes in the power of incident light. The oscillatory frequency and values of  $1/\tau_1$  and  $1/\tau_3$  increased with increasing light intensity, whereas each value of  $\tau_2$  and  $\tau_4$  for the assembly remained constant at  $3 \pm 1\text{ ms}$  (Figure S3).

Self-oscillatory motion was generally observed in thin plate-like crystals of various shapes under continuous 435-nm light irradiation in a four-step manner<sup>[19]</sup> (Figure 5b). The magnitude of displacement and time ( $\tau$ ) for each step differed from those of the assembly in Figure 5a. However, similarly to the time profile in Figure 5a, both  $1/\tau_1$  and  $1/\tau_3$  were proportional to the applied light intensity (slopes in Figure 5d are 1), whereas  $\tau_2$  and  $\tau_4$  remained constant when the irradiation intensity was changed. These results indicate that S1 and S3 are one-photon processes. In contrast, the motions

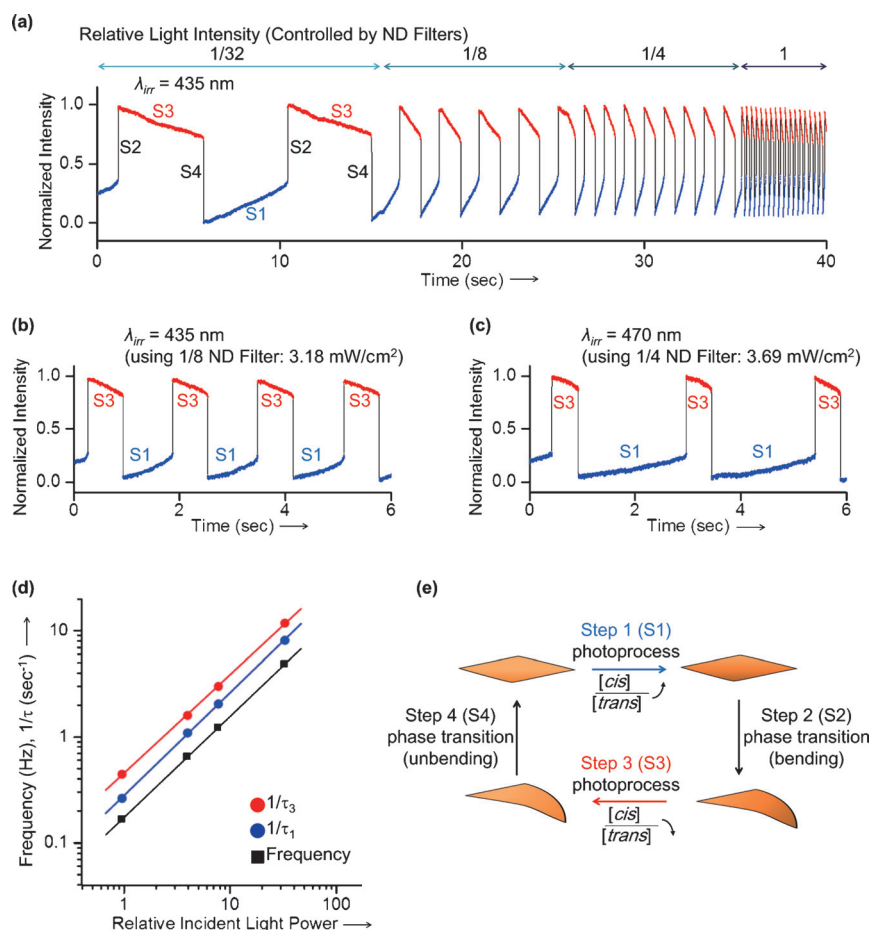


**Figure 5.** Time profiles of self-oscillations. Each intensity on the vertical axis was determined from the brightness change of a region of the assembly recorded by the microscope (20× objective lens) and normalized using the two extreme values. a) Time profile of self-oscillation of a crystalline assembly under various intensities of incident light (Movie S2). b, c) Time profiles of self-oscillations of another crystalline assembly under b) 435-nm light and c) 470-nm light. d) Frequency and time spans of S1 and S3 as a function of intensity of 435-nm light for the crystalline assembly in (b). Slopes indicate that S1 and S3 are one-photon processes. e) Schematic illustration of each step (S1–S4) of the self-oscillatory motion.

of S2 and S4 are not directly induced by individual photons, but by the intrinsic structures of the assemblies.

The in situ SAXRD profile of crystalline assemblies in aqueous dispersion was measured under 455-nm light irradiation with a handheld LED lamp ( $\lambda$  span = 445–485 nm) (Figure 3b). Because the exposure time (60 min) far exceeded the oscillation cycle period, the structures of the S1 and S3 states could both be detected. Two peaks appeared, one of which was assigned to the original crystalline phase ( $d = 4.6\text{ nm}$ ). The other peak ( $d = 4.0\text{ nm}$ ,  $q = 1.59\text{ nm}^{-1}$ ), which developed under blue-light irradiation, represented the other polymorphic phase of a bi-stable crystal under irradiation. This crystalline sample showed self-oscillatory motion under 435-nm light irradiation, both before and after the SAXRD measurement.

The HPLC experiment revealed that the percentages of **1-trans** and **1-cis** in the synthesized crystalline assembly were 99.8% and 0.2%, respectively, in the dark (Figure 4b). In a methanolic solution, the steady-state ratio of **1-trans** to **1-cis**

under continuous 455-nm light irradiation with the handheld LED was 75:25 (Figure 4d). Under the same light-irradiation condition, the ratio in the crystalline assemblies was 96.5:3.5, which is the average ratio of **1-trans** and **1-cis** while the crystals are oscillating (Figure 4c). One reason for the difference in ratios between the methanolic solution and crystalline assemblies is that the regular packing of molecules in the crystal inhibits *cis*-isomer formation (as discussed in depth elsewhere).<sup>[20]</sup> The strength of the inhibition differs across two distinguishable polymorphic phases, owing to the difference in the molecular packing of the phase.

In methanolic solution, ratios of the absorption coefficients of **1-trans** to **1-cis** were larger at 435 nm than at 470 nm (see Table 1), whereas the quantum yields of photoisomerization were equivalent. Assuming that the relationships of **1** and **2** remain as they are in the crystalline phase, the kinetic ratio of the *trans*-to-*cis* to *cis*-to-*trans* isomerization should be larger under 435- than under 470-nm light. Figure 5c shows the time profile of the same assembly as shown in Figure 5b, but under 470-nm light irradiation.<sup>[21]</sup> The increased  $\tau_1$  to  $\tau_3$  ratio under 470-nm light irradiation indicates that there is a net *trans*-to-*cis* isomerization in S1 and, conversely, a net *cis*-to-*trans* isomerization in S3. This switching process is discussed in detail in the Supporting Information.

The self-oscillation dynamics can be summarized as follows (Figure 5e). In S1, the photoreaction increases the population of *cis*-isomer. However, due to instability of the original phase with increased *cis*-isomer levels, the morphology of the crystalline assembly changes in S2. Subsequently, the photoreaction decreases the population of *cis*-isomer in S3. This decrease likely is due to a change in the photoisomerization quantum yield, owing to the molecular arrangement in the new polymorphic phase. Alternatively, the *cis*-isomer decrease might be due to an increase in the absorption cross-section ratio of *cis*- compared to *trans*-isomer in the new polymorphic phase. When the *trans*-isomer fraction reaches a threshold, the assembly returns to its original morphology because of the stability of the original crystalline phase, which is characterized by a small portion of *cis*-isomer, in S4. By repeating this cycle, the crystalline assembly shows square-wave periodic self-oscillation with a constant amplitude and light intensity-dependent frequency.

The macroscopic self-oscillation reported herein is a type of autonomous limit-cycle oscillation that shows repeated flips in a steady manner under continuous photoirradiation. Oscillation parameters, such as amplitude and frequency, depend on the properties (e.g., thickness) of individual assemblies (Movie S3). Previously reported photo-driven oscillators have been intrinsically limited in their flipping direction by the orientation and polarization of the external light source.<sup>[11]</sup> By contrast, the self-oscillation presented herein is realized by an autonomous combination of a change of photoisomerization efficiency and phase transitions of the molecular assembly. This bi-stable switching mechanism may be widely and universally applicable for producing macroscopic molecular motors that function in temporally multimodal frequencies with spatially organized motions by arranging the shapes and components of the assemblies. As shown in Movie S4, a frog-kick motion of a waving ribbon

composed of **1**, **2**, and stearic acid was realized.<sup>[22]</sup> Moreover, because the bi-stability switching reaction is not limited to photoisomerization, this mechanism has potential utility for the creation of autonomous motors triggered by a wide range of chemical machines. The importance of this study lies in the realization of macroscopic self-oscillation by the repeated reversible reaction of a molecular machine with the cooperative transformation of a molecular assembly. These results provide a fundamental strategy for constructing dynamic self-organizations in supramolecular systems to achieve bioinspired molecular systems.<sup>[1,23]</sup>

## Acknowledgements

This work was funded by JST PRESTO (Molecular Technology). The SAXRD experiment was carried out at the CRIS OPEN FACILITY (Hokkaido Univ.).

**Keywords:** cooperative effects · molecular devices · non-equilibrium processes · phase transitions · photochromism

**How to cite:** *Angew. Chem. Int. Ed.* **2016**, *55*, 8239–8243  
*Angew. Chem.* **2016**, *128*, 8379–8383

- [1] a) E. R. Kay, D. A. Leigh, *Angew. Chem. Int. Ed.* **2015**, *54*, 10080–10088; *Angew. Chem.* **2015**, *127*, 10218–10226; b) J.-M. Lehn, *Angew. Chem. Int. Ed.* **2015**, *54*, 3276–3289; *Angew. Chem.* **2015**, *127*, 3326–3340; c) E. Mattia, S. Otto, *Nat. Nanotechnol.* **2015**, *10*, 111–119; d) M. von Delius, D. A. Leigh, *Chem. Soc. Rev.* **2011**, *40*, 3656–3676; e) B. A. Grzybowski, C. E. Wilmer, J. Kim, K. P. Browne, K. J. M. Bishop, *Soft Matter* **2009**, *5*, 1110–1128; f) M. Orlik, *J. Solid State Electrochem.* **2009**, *13*, 245–261; g) E. R. Kay, D. A. Leigh, F. Zerbetto, *Angew. Chem. Int. Ed.* **2007**, *46*, 72–191; *Angew. Chem.* **2007**, *119*, 72–196; h) W. R. Browne, B. L. Feringa, *Nat. Nanotechnol.* **2006**, *1*, 25–35.
- [2] V. Balzani, A. Credi, M. Venturi in *Molecular Devices and Machines—A Journey into the Nanoworld*, Wiley-VCH, Weinheim, **2003**.
- [3] a) P. Naumov, S. Chizhik, M. K. Panda, N. K. Nath, E. Boldyreva, *Chem. Rev.* **2015**, *115*, 12440–12490; b) T. Ube, T. Ikeda, *Angew. Chem. Int. Ed.* **2014**, *53*, 10290–10299; *Angew. Chem.* **2014**, *126*, 10456–10465; c) A. Priimagi, C. J. Barrett, A. Shishido, *J. Mater. Chem. C* **2014**, *2*, 7155–7162; d) T. Aida, E. W. Meijer, S. I. Stupp, *Science* **2012**, *335*, 813–817; e) A. Natansohn, P. Rochon, *Chem. Rev.* **2002**, *102*, 4139–4175.
- [4] a) S. Iamsaard, S. J. Abhoff, B. Matt, T. Kudernac, J. J. L. M. Cornelissen, S. P. Fletcher, N. Katsonis, *Nat. Chem.* **2014**, *6*, 229–235; b) M. Baroncini, C. Gao, V. Carboni, A. Credi, E. Previtera, M. Semeraro, M. Venturi, S. Silvi, *Chem. Eur. J.* **2014**, *20*, 10737–10744; c) L. Osorio-Planes, M. Espelt, M. A. Pericàs, P. Ballesster, *Chem. Sci.* **2014**, *5*, 4260–4264.
- [5] Y. Kageyama, N. Tanigake, Y. Kurokome, S. Iwaki, S. Takeda, K. Suzuki, T. Sugawara, *Chem. Commun.* **2013**, *49*, 9386–9388.
- [6] a) R. Eelkema, M. M. Pollard, J. Vicario, N. Katsonis, B. S. Ramon, C. W. M. Bastiaansen, D. J. Broer, B. L. Feringa, *Nature* **2006**, *440*, 163; b) J. Berná, D. A. Leigh, M. Lubomska, S. M. Mendoza, E. M. Pérez, P. Rudolf, G. Teobaldi, F. Zerbetto, *Nat. Mater.* **2005**, *4*, 704–710; c) Y. Liu, A. H. Flood, P. A. Bonvallet, S. A. Vignon, B. H. Northrop, H.-R. Tseng, J. O. Jeppesen, T. J. Huang, B. Brough, M. Baller, S. Magonov, S. D. Solares, W. A. Goddard, C.-M. Ho, J. F. Stoddart, *J. Am. Chem. Soc.* **2005**, *127*, 9745–9759.

- [7] a) P. Glansdorff, I. Prigogine, *Physica* **1964**, *30*, 351–374; b) G. Nicolis, I. Prigogine, in *Self-Organization in Nonequilibrium Systems: From Dissipative Structures to Order through Fluctuations* (Japanese Transl. Iwanami, **1980**), Wiley, New York, **1977**.
- [8] For examples, a) T. Rungsimanon, K. Yuyama, T. Sugiyama, H. Masuhara, *Cryst. Growth Des.* **2010**, *10*, 4686–4688; b) H. Kitahata, K. Kawata, Y. Sumino, S. Nakata, *Chem. Phys. Lett.* **2008**, *457*, 254–258.
- [9] A. Zaikin, A. M. Zhabotinsky, *Nature* **1970**, *225*, 535–537.
- [10] a) “Self-oscillating polymer gels”: R. Yoshida in *Supramolecular Soft Matter* (Eds.: T. Nakanishi), Wiley, Hoboken, **2011**, chap. 12; b) H. Zhou, Z. Zheng, Q. Wang, G. Xu, J. Li, X. Ding, *RSC Adv.* **2015**, *5*, 13555–13569.
- [11] a) S. Serak, N. Tabiryan, R. Vergara, T. J. White, R. A. Vaia, T. J. Bunning, *Soft Matter* **2010**, *6*, 779–783; b) T. J. White, N. V. Tabiryan, S. V. Serak, U. A. Hrozhyk, V. P. Tondiglia, H. Koerner, R. A. Vaia, T. J. Bunning, *Soft Matter* **2008**, *4*, 1796–1798.
- [12] X. L. Jiang, L. Li, J. Kumar, D. Y. Kim, V. Shivshankar, S. K. Tripathy, *Appl. Phys. Lett.* **1996**, *68*, 2618–2620.
- [13] Y. Tabe, H. Yokoyama, *Langmuir* **1995**, *11*, 4609–4613.
- [14] G. Ragazzon, M. Baroncini, S. Silvi, M. Venturi, A. Credi, *Nat. Nanotechnol.* **2015**, *10*, 70–75.
- [15] Wide-range XRD profile of the crystalline assembly is shown in Figure S2.
- [16] After drying, the hydrated crystalline assembly was transformed into the other phase under ambient atmosphere. Therefore, X-ray single-crystal analysis was not able to be carried out successfully.
- [17] The structure of the helical assembly of oleic acid was revealed to be an inverted hexagonal assembly. Details are reported in Y. Kageyama, T. Ikegami, N. Hiramatsu, S. Takeda, T. Sugawara, *Soft Matter* **2015**, *11*, 3550–3558.
- [18] Self-oscillatory motion was also observed under focused light from the 455-nm handheld LED lamp. Dehydrated crystalline assemblies did not show any motion under 435-, 455-, or 470-nm light irradiation.
- [19] Most of the thin plate-like crystals showed self-oscillation in a four-step manner. On the other hand, some crystals having large areas or complex structures showed multistep oscillation.
- [20] a) L. Xing, W. L. Mattice, *Langmuir* **1996**, *12*, 3024–3030; b) M. Matsumoto, S. Terrettaz, H. Tachibana, *Adv. Colloid Interface Sci.* **2000**, *87*, 147–164.
- [21] Under 470-nm light, S1 and S3 were also one-photon processes, as shown in Figure S4.
- [22] Self-oscillatory motion was observed regularly in the thin-plate crystalline assemblies of **1** and **2**. Some crystalline assemblies composed of **1** and other fatty acids, such as stearic acid and palmitoleic acid, showed various self-oscillatory motions, such as waving, rowing, and blowing motions. In our study, no macroscopic oscillations were observed in crystals of **1** without fatty acids. Detailed studies of these processes are ongoing.
- [23] a) K. Ruiz-Mirazo, C. Briones, A. Escosura, *Chem. Rev.* **2014**, *114*, 285–366; b) J. R. Nitschke, *Nature* **2009**, *462*, 736–738.

Received: January 8, 2016

Revised: March 9, 2016

Published online: May 19, 2016